

# High-loop perturbative renormalization constants for Lattice QCD (I): finite constants for Wilson quark currents.

F. Di Renzo <sup>a</sup>, V. Miccio <sup>b</sup>, C. Torrero <sup>c</sup> and L. Scorzato <sup>d</sup>

<sup>a</sup> *Dipartimento di Fisica, Università di Parma  
and INFN, Gruppo Collegato di Parma, Italy*

<sup>b</sup> *I.N.F.N., Sezione di Milano Bicocca, Italy*

<sup>c</sup> *Faculty of Physics, University of Bielefeld, Germany*

<sup>d</sup> *ECT\*, Villazzano (Trento), Italy*

## Abstract

We present a high order perturbative computation of the renormalization constants  $Z_V$ ,  $Z_A$  and of the ratio  $Z_P/Z_S$  for Wilson fermions. The computational setup is the one provided by the *RI'-MOM* scheme. Three- and four-loop expansions are made possible by Numerical Stochastic Perturbation Theory. Results are given for various numbers of flavours and/or (within a finite accuracy) for generic  $n_f$  up to three loops. For the case  $n_f = 2$  we also present four-loop results. Finite size effects are well under control and the continuum limit is taken by means of *hypercubic symmetric Taylor expansions*. The main indetermination comes from truncation errors, which should be assessed in connection with convergence properties of the series. The latter is best discussed in the framework of Boosted Perturbation Theory, whose impact we try to assess carefully. Final results and their uncertainties show that high-loop perturbative computations of Lattice QCD RC's are feasible and should not be viewed as a second choice. As a by-product, we discuss the perturbative expansion for the critical mass, also for which results are for generic  $n_f$  up to three loops, while a four-loop result is obtained for  $n_f = 2$ .

# 1 Introduction

Lattice Perturbation Theory (LPT) has been for a long time the only available tool for the computation of Lattice QCD Renormalization Constants (RC's). By now it is usually not even held as the major one any more. One should stress that there is no theoretical obstacle to the perturbative computation of either *finite* or *logarithmically divergent* RC's like, for example, those for quark bilinears or ratios of them. As a matter of fact, there are actually many practical obstacles. The very first one is that LPT is technically very hard, actually by far harder than Perturbation Theory (PT) on the continuum [1]. It thus does not come as a surprise that computations are often only performed at one loop. This is a serious limitation, which is made even more severe by the bad convergence properties of LPT. To take care of this problem large use is made of the so-called Boosted Perturbation Theory (BPT) and/or of the so-called Tadpole-Improved Perturbation Theory (TIPT) [2]. There is quite a consensus on the fact that, given a one loop LPT computation, the impact of BPT (and/or TIPT) is often quite important. On the other side, there is no clear-cut result on the actual control on these procedures. One should always keep in mind that convergence properties of the series are the real issue and assessing them from a BPT (or TIPT) one-loop computation is of course impossible. Other improvement schemes have been in recent years proposed, which aim at resumming some leading contributions [3].

Even if there are effects that can be resummed, any perturbative computation is necessarily a finite-order computation and in the end one always has to live with truncation errors. This is also true for the high-order computations that can be performed in the continuum. One is nevertheless aware of the fact that there are regimes in which it is the theory itself which enables one to safely make use of PT. As already stated, this is just the case of logarithmically divergent (or even finite) RC's for QCD, whose coupling is small in a convenient regime.

Living with truncation errors at one loop is anyway quite a hard life. This motivated the many progresses which in recent years came from a completely non-perturbative approach to the computation of RC's in Lattice QCD. One needs to make use of an intermediate scheme, which is eventually matched to the  $\overline{\text{MS}}$  scheme (the one in which phenomenologists are most interested in) by a continuum perturbative computation. Popular intermediate schemes are *RI'-MOM* [4] and *SF* [5].

While by a non-perturbative computation one in principle gets rid of truncation errors, on the other side one needs to confront all the difficulties which are inherent in numerics. Among these one should of course quote the high computational effort which is peculiar of unquenched (or, better, partially quenched) Lattice QCD simulations. There are actually computations which are in principle possible, but in practice (at the best) very difficult.

This is the main reason why LPT is still a tool one can not live without. Either to guide the hand in cases in which non-perturbative computations are still under their way or to give an answer in cases for which non-perturbative computations at the moment are not addressable, in the end one has to revert to LPT.

In recent years the technique of Numerical Stochastic Perturbation Theory (NSPT) has been introduced (for a quite extended introduction - which in particular covers the un-

quenched version - see [6]). NSPT is a numerical implementation of Stochastic PT [7]. It is a numerical tool which enables to perform LPT computations with no reference whatsoever to diagrammatics.

By making use of NSPT we can compute Lattice QCD RC's to high orders, which in the context of the present work means 3 (or even 4) loops. At these orders the use of BPT enables one to assess convergence properties of the series and so to take quite a good control on truncation errors. Dealing with a numerical method, one has to stick to finite-volume computations, so that finite-volume effects have to be carefully assessed: this can be done. A careful extraction of continuum limit is one of the good point of the approach: the solution comes from what we call *hypercubic symmetric Taylor expansions*. Another nice feature comes from the fact that staying in the massless limit in which RC's are often defined does not require any extrapolation procedure.

The main message of this paper is that high-loop perturbative computations of Lattice QCD RC's are feasible and should not be viewed as a second choice. In particular, when one has at hand both a perturbative and a non-perturbative determination of a RC, it is of course valuable to make a comparison. This is not at all academic. As a matter of fact, non-perturbative determinations are based on assumptions that are actually only proved in PT. On top of that, one should keep in mind that non-perturbative computations are limited to fixed values for the coupling and the number of flavours.

This is the first of a couple of papers which deal with the NSPT perturbative computation of Wilson quark bilinears, with renormalization conditions fixed by the *RI'-MOM* prescriptions. Notice that we are in a position to make comparison with a non-perturbative determination [8].<sup>1</sup> In this paper we will in particular concentrate on the determination of *finite* RC's:  $Z_V$ ,  $Z_A$  and the ratios  $Z_P/Z_S$  and  $Z_V/Z_A$ <sup>2</sup> for (unimproved) Wilson fermions. As a by-product, we also obtain the expansion for the critical mass. Results are given for various numbers of flavours. At three loops some results are even given (to a finite accuracy) for generic  $n_f$ , while we present fourth loop results for the  $n_f = 2$  case. A different paper will deal with the computation of logarithmically divergent RC's for quark bilinears (in particular, the RC for the scalar current  $Z_S = Z_m^{-1}$ , which is phenomenologically relevant for the determination of the quark masses). This deserves some extra caution since dealing with anomalous dimensions requires a peculiar care for finite volume effects.

The paper is organized as follows. In section 2 we recall the basic definitions of the renormalization scheme to which we adhere, while in section 3 we discuss some technical details of our computations. Section 4 introduces the main tool which is needed to extract the continuum limit (the already mentioned *hypercubic symmetric Taylor expansions*): this is done by discussing the (prototype) computation of the quark propagator. Section 5 contains our results: first we discuss the finite ratios  $Z_P/Z_S$  and  $Z_V/Z_A$ , for which we can fit three loops results for generic  $n_f$ ; then we move to  $Z_V$  and  $Z_A$  (results are given at three loops for  $n_f = 0$  and at four loops for  $n_f = 2$ ); finally we present a by-product of our computations, *i.e.* the critical mass to three loops (again, actually four in the case  $n_f = 2$ ). In section 6 we discuss the general features of computations dealing with an anomalous dimension (this sets the stage for what will be discussed in a following paper [9]). In section 7 we deal with

---

<sup>1</sup>The comparison will be made for given values of the coupling ( $\beta = 5.8$ ) and number of flavours ( $n_f = 2$ ).

<sup>2</sup>We will see in what sense we regard the computation of  $Z_V$ ,  $Z_A$  and  $Z_V/Z_A$  as non tautological.

resummations and convergence properties of our series and finally section 8 contains our conclusions and perspectives for future applications.

## 2 The RI'-MOM renormalization scheme

In order to compute renormalization constants we adhere to the *RI'-MOM* scheme. This is one of the so-called physical schemes<sup>3</sup> (as opposed to the more popular  $\overline{\text{MS}}$  scheme) and has got quite a long history, going back to the *MOM* scheme of [10]. It became very popular after the introduction of non-perturbative renormalization in [4]. *RI* emphasizes the *regulator independent* nature of the scheme, which in particular makes the lattice a viable regulator. The prime reminds us of a renormalization condition for the quark field which is slightly different from the original one. All the details on the scheme can be found elsewhere, for example in [11]. In the following we simply introduce the definitions which are relevant for our application.

The basic building block is the computation of quark bilinears between external quark states at fixed (off-shell) momentum  $p$

$$\int dx \langle p | \bar{\psi}(x) \Gamma \psi(x) | p \rangle = G_\Gamma(pa). \quad (1)$$

Here  $\Gamma$  stands for any of the 16 matrices providing the standard basis in the Dirac space (Dirac indexes here and several times in the following will be suppressed), thus singling out one of the  $S$  (scalar),  $V$  (vector),  $P$  (pseudoscalar),  $A$  (axial),  $T$  (tensor) currents. The dependence on  $pa$  (which we will often write in the following  $\hat{p} = pa$ ) displays that the lattice is to be intended as the regulator in our computations.

Being these quantities gauge-dependent, a choice for the gauge condition has to be made. We will focus on computations in the Landau gauge. From a numerical point of view, this gauge condition is easy to fix on the lattice. On top of that, one does not need to discuss the gauge parameter renormalization. It also gives some extra bonus: the anomalous dimension for the quark field is zero at one loop.

One then trades the  $G_\Gamma(pa)$  for the amputated function, which we write  $\Gamma_\Gamma(pa)$  ( $S(pa)$  is the quark propagator)

$$G_\Gamma(pa) \rightarrow \Gamma_\Gamma(pa) = S^{-1}(pa) G_\Gamma(pa) S^{-1}(pa). \quad (2)$$

The  $\Gamma_\Gamma(pa)$  are eventually projected on the tree-level structure by a suitable operator  $\hat{P}_{O_\Gamma}$

$$O_\Gamma(pa) = \text{Tr} \left( \hat{P}_{O_\Gamma} \Gamma_\Gamma(pa) \right). \quad (3)$$

Renormalization conditions are now given in terms of the  $O_\Gamma(pa)$  according to

$$Z_{O_\Gamma}(\mu a, g(a)) Z_q^{-1}(\mu a, g(a)) O_\Gamma(pa) \Big|_{p^2=\mu^2} = 1. \quad (4)$$

Here the dependence of the  $Z$ 's on the scale  $\mu$  is via the dimensionless quantity  $\mu a$ , while the dependence on  $g(a)$  explicitly displays that our results will be expansions in the lattice

---

<sup>3</sup>One should nevertheless keep in mind that the name *physical* is actually misleading in the case of QCD.

coupling. One should keep in mind from the very beginning that we will be eventually interested in the  $a \rightarrow 0$  limit of the  $Z$ 's. The quark field renormalization constant  $Z_q$  which enters the above formula is defined by

$$Z_q(\mu a, g(a)) = -i \frac{1}{12} \frac{\text{Tr}(\not{p} S^{-1}(pa))}{p^2} \Big|_{p^2=\mu^2}. \quad (5)$$

This is the already-mentioned difference with respect to the original *RI* scheme, for which the definition of  $Z_q$  implies a derivative with respect to  $p^\mu$ .

In order to get a mass-independent renormalization scheme, one imposes renormalization conditions on massless quarks. In Perturbation Theory this implies the knowledge of the relevant counterterms, *i.e.* the values of the various orders of the Wilson fermions critical mass. One- and two-loop results are known from the literature [12]. Third (and fourth) loop have been computed by us as a (necessary) by-product of the current computations: results are reported in section 5 (the three loop result in the  $n_f = 2$  case has already been reported in [6]). Notice that the situation in the non-perturbative framework is more cumbersome with respect to staying in the massless limit. The determination of the critical mass is in a sense the prototype non-perturbative computation of a(n additive) renormalization constant. As it is well known, this is also a matter of principle: being a power-divergent renormalization, the critical mass itself can not be computed in Perturbation Theory in the continuum limit. Still, from a numerical point of view the massless limit is always reached by an extrapolation procedure, which is usually a major source of error in non-perturbative determinations of RC's for Lattice QCD.

A great advantage of working in the *RI'-MOM* scheme is that the relevant anomalous dimensions are known to 3 loops [11]. One is usually ready to admit that getting the logarithms is the *easy* part in the computation of a renormalization constant, while fixing the finite parts is the *hard* part of the work. As we will see, the situation is to a certain extent the opposite in the case of NSPT. We actually take for granted the logarithms (they are fixed by the choice of the scheme) and mainly concentrate on the computation of finite parts. As it is discussed in section 6, finite size effects open anyway the backdoor to corrections to the logarithmic contributions. Being 3 loops the order to which anomalous dimensions are known, this is also the order at which we can push our computations for every observable which has a non-vanishing anomalous dimension. On the other side, the finite RC's we will be concerned with in the present paper are in principle not constrained by anything but numerical precision, and that is why we pushed the computation of these quantities to an even higher order (4 loops, at the moment).

### 3 Some technical details of our computations

The lattice formulation we adhere to is that of plain Wilson action for gauge fields and plain (*i.e.* unimproved) Wilson fermions. As for our computational tool (NSPT), here it suffices to point out the technical details which are relevant to the computation at hand. In its actual implementation, NSPT shares a few ingredients which are common to any lattice simulation. The main peculiarity is the representation of the fields as an expansion in the

coupling constant, *i.e.*

$$U_\mu(x) = 1 + \sum_{i=1}^N \beta^{-\frac{i}{2}} U_\mu^{(i)}(x) . \quad (6)$$

As it is apparent from the formula above, our preferred expansion parameter is the inverse of the lattice parameter  $\beta = 2N_C/g_0^2$ ,  $N_C$  being the number of colors and  $g_0 = g(a)$  the bare lattice coupling; thus  $\beta^{-\frac{1}{2}}$  is the counterpart for  $g_0$ . In our case a three-loop computation requires  $N = 6$ , while for four loops (which is at the moment the maximum order for which we report results in the  $n_f = 2$  case) one needs  $N = 8$ . The proliferation of fields results in the request of a bigger amount of memory than in ordinary (non-perturbative) lattice QCD simulations. It is of course relevant also in terms of computing power: the algorithm is dominated by order-by-order multiplications, *i.e.* the number of floating-point operations grows as  $N(N + 1)/2$ . While this could appear as a big overhead with respect to ordinary non-perturbative dynamics, this is actually not true. In particular, in unquenched NSPT (like in any fermionic simulation) the basic building block is the inversion of the Dirac matrix, for which the perturbative nature of the computation results in a *closed* recursive algorithm, which is fairly well implemented (see [6]). On top of that, as we will discuss a bit more later, there is no need for an extrapolation to the chiral limit. As a result, NSPT fermionic computations are actually less demanding than non-perturbative counterparts.

As in many non-perturbative numerical computations, it is worth producing fairly decorrelated configurations and store them for different subsequent measurements. A  $32^4$  lattice (both at three and at four loops) fits well on an *APEmille* crate. At the same orders, a  $16^4$  lattice can be managed by small *PC*-clusters or even by a robust (but nowadays standard) *PC*. While the first case is treated by our *TAO*<sup>4</sup> codes, the second is implemented in the framework of a by now well-established *C<sup>++</sup>* NSPT package.

The number of flavours  $n_f$  enters the computations as a parameter, *i.e.* one has to perform different simulations for different  $n_f$ 's. In Perturbation Theory each order has a trivial polynomial dependence on  $n_f$ , so that one can fit the  $n_f$  dependence.  $n_f = 0$  has by now been simulated both on  $16^4$  and on  $32^4$  lattices: results have been used to assess finite-size effects. The unquenched cases have been simulated on the bigger ( $32^4$ ) lattice:  $n_f = 2$  is the case for which we have the largest number of configurations, while we also have several tenths of configurations for both  $n_f = 3$  and  $n_f = 4$ . As a result, at the moment we are not going to quote every result for any  $n_f$ . In particular, four-loop results are at the moment only given in the case  $n_f = 2$ , for a reason that will be clear in a moment.

As already stated, one good feature of NSPT computations is the fact that one can stay at the chiral limit. As we have already pointed out, the computation of the Wilson fermion critical mass was in a sense the prototype computation of a non-perturbative (additive, in this case) renormalization constant. It is also the prototype of a power-divergent renormalization, which can not be safely computed in PT in the continuum limit. On the other hand, no numerical simulation can be performed at  $k_{critical}$  (we adhere to the common non-perturbative notation of quoting the hopping parameter rather than the mass of the quark): the chiral limit is always reached by means of a convenient chiral extrapolation.

---

<sup>4</sup>*TAO* is the *APE*-dedicated programming language.

In Perturbation Theory one corrects for the additive quark mass renormalization by plugging in critical mass counterterms order by order. This is exactly what we do in NSPT. We were ready to start our simulations straightaway at three-loop order, which requires the knowledge of the critical mass up to two loops, and this is exactly what can be taken from the literature [12]. Each subsequent order asks for an iterative procedure: one computes the critical mass at the  $n^{th}$  order (from  $n^{th}$ -order simulations) and then plug it in the  $(n+1)^{th}$ -order simulations. In particular, for the case  $n_f = 2$  our determination of the three-loop critical mass was good enough to plug it into four-loop simulations. The statistics we collected for the other values of  $n_f$  are at the moment not sufficient to safely aim at the same accuracy.

The *RI'-MOM* scheme renormalization has been discussed in a generic covariant gauge [11]. We have already stated that our computations were performed in Landau gauge and stressed what the advantages of a such a choice are. From the point of view of computer simulations fixing the gauge to Landau in NSPT simply requires the order-by-order implementation of a well-known (*FFT*-accelerated) iterative procedure (for details, see [6]). It is worth stressing that in the NSPT framework also a peculiar implementation of the Faddeev-Popov mechanism is possible (see [13] for an application): by the same trick which enables us to treat the fermionic determinant we can manage the Faddeev-Popov determinant, without the inclusion of ghost fields. Still, we can compute in any covariant gauge with gauge parameter  $\xi \neq 0$ , *i.e.* Landau gauge is the only one which is not viable (apart from an extrapolation procedure). While the generic covariant gauge NSPT simulation has a (moderate) computational overhead, Landau gauge-fixing has a delicate issue in the numerical noise which is introduced by the (order-by-order) iteration. We explicitly checked that this noise was not a big problem (of course *FFT*-acceleration is quite helpful in reducing the number of iterations needed to fix the gauge). In the end the advantages of computing in Landau gauge were not overtaken by the care that is due to keep this noise under control.

We now come to briefly describe how we compute the observables of Eq. (1). Trivial algebra (*i.e.* creating external states with quark operators and Wick-contracting to obtain propagators) leaves us with the task of computing expectation values (*i.e.* asymptotic Langevin time averages) of the quantities ( $M$  is the Dirac operator and  $\alpha$  and  $\beta$  the external polarizations; color degrees of freedom are always suppressed in the notation)

$$\sum_{q;\sigma\tau} M_{\alpha\sigma}^{-1}(p, q) \Gamma_{\sigma\tau} M_{\tau\beta}^{-1}(q, p). \quad (7)$$

The index  $p$  in the inverse Dirac operator is singled out by placing a  $\delta$ -like source at  $p$  in momentum space, with the right polarization and color index (more details in the following section). Notice that in this way not only the inverse is to be computed on a source (as usual), but one actually squeezes all the information out of the configuration. This is the advantage of working directly in momentum space, which is natural in our framework (every inversion of  $M$  comes as a result of a computation which goes back and forth from momentum space; again, see [6] for details). The only measurement which is a bit different is that of the conserved vector current

$$V_\mu^c = 1/2 \left( \bar{\psi}(x) (\gamma_\mu - 1) U_\mu(x) \psi(x + \mu) + \bar{\psi}(x + \mu) (\gamma_\mu + 1) U_\mu^\dagger(x) \psi(x) \right). \quad (8)$$

A little algebra shows that also in this case the measurement can be quite efficient by reverting to a convolution product.

A very important improvement of our statistics comes from exploiting hypercubic symmetry: all the measurements connected by a hypercubic symmetry transformation are averaged. The fluctuations associated to this average are taken into account for assessing errors. As a general rule for the different measurements involved in our calculations, bootstrap was the basic tool for the computation of errors.

## 4 Hypercubic symmetric Taylor expansions: the case of the quark propagator

We now proceed to discuss in detail a prototype computation, *i.e.* the one loop computation of the quark field renormalization constant. From a more practical point of view, we are going to describe how we measure the quark propagator. We will thus make clear what we mean by *hypercubic symmetric Taylor expansions*.

The section is intended as a prototype computation, so let us pin down in general what the expected form of the  $L^{\text{th}}$  loop coefficient of a RC is:

$$z_L = c_L + \sum_{i=1}^L d_i(\gamma) \log(\hat{p})^i + F(\hat{p}) \quad (\hat{p} = pa). \quad (9)$$

We have to look for a finite number ( $c_L$ ), a divergent part which is a function of anomalous dimensions  $\gamma$ 's and irrelevant pieces, which we can expect compliant to hypercubic symmetry and described by a suitable function  $F$ . Our strategy requires that the anomalous dimensions which we need are taken from the literature and their contribution is subtracted. In particular, for a one-loop computation one simply needs to subtract a simple  $\log$  multiplied by the one-loop anomalous dimension (in this section we will completely ignore all the contributions coming from finite-size effects, to which we will come back in Section 6). After such a subtraction we need a convenient way to fit the irrelevant pieces given by  $F(\hat{p})$ . The example at hand is both instructive and simple: in particular, in Landau gauge the quark field has zero anomalous dimension at one loop, so it is simply required that we get rid of  $F(\hat{p})$  in order to get the constant  $c_L$  we are interested in.

We need to compute the two points vertex function (the inverse of the quark propagator). We specify our computation to a massless fermion; in the continuum limit

$$\Gamma_2(p^2) = S(p^2)^{-1}.$$

Let us specify the notation to our lattice regularized computation, which in first instance deals with dimensionless quantities. Just like in  $\hat{p} = pa$ , we use the *hat* notation for other dimensionless quantities; furthermore, we also explicitly write the dependence on the coupling (and since we compute in PT we write  $\beta^{-1}$  rather than  $\beta$ )

$$\begin{aligned} \Gamma_2(\hat{p}, \hat{m}_{cr}, \beta^{-1}) &= S(\hat{p}, \hat{m}_{cr}, \beta^{-1})^{-1} \\ &= i \hat{p} + \hat{m}_W(\hat{p}) - \Sigma(\hat{p}, \hat{m}_{cr}, \beta^{-1}) \end{aligned} \quad (10)$$

where  $\hat{m}_W(\hat{p}) = \mathcal{O}(\hat{p}^2)$  is the (irrelevant) mass term generated at tree level by the Wilson prescription,  $\Sigma(\hat{p}, \hat{m}_{cr}, \beta^{-1})$  is the self-energy (which is  $\mathcal{O}(\beta^{-1})$ ) and  $\hat{m}_{cr}$  is the critical

mass (which is  $\mathcal{O}(\beta^{-1})$  as well): here we finally read in a formula that due to the Wilson regularization, even if the bare mass is zero, one needs mass counterterms to stay at zero renormalized mass. Notice that  $\hat{m}_{cr}$  is still a dimensionless quantity. The self energy can in turn be written

$$\Sigma(\hat{p}, \hat{m}_{cr}, \beta^{-1}) = \Sigma_c(\hat{p}, \hat{m}_{cr}, \beta^{-1}) + i \not{p} \Sigma_V(\hat{p}, \hat{m}_{cr}, \beta^{-1}). \quad (11)$$

$\Sigma_c$  is the contribution along the (Dirac) identity operator, which is the one contributing to the computation of the critical mass according to the definition

$$\Sigma(0, \hat{m}_{cr}, \beta^{-1}) = \Sigma_c(0, \hat{m}_{cr}, \beta^{-1}) = \hat{m}_{cr} = a m_{cr}. \quad (12)$$

By restoring physical dimensions one can inspect the  $a^{-1}$  divergence of the critical mass:  $a^{-1} \Sigma_c(0, \hat{m}_{cr}, \beta^{-1}) = m_{cr}$ . We will come back to it in the following section. For the moment being, we will concentrate on the other contribution, from which the quark field RC is extracted.

First of all we compute  $S(\hat{p}, \hat{m}_{cr}, \beta^{-1})$ , *i.e.*

$$S(\hat{p}, \hat{m}_{cr}, \beta^{-1})_{\alpha\eta} = \langle M_{\alpha\eta}^{-1}(p, p) \rangle = T^{-1} \sum_{t=1}^T M_{\alpha\eta}^{-1}(p, p|t).$$

Three comments are in order concerning the previous formula. We explicitly show how expectation values come from averages over a number of configurations, which in turns have to be regarded as averages over a long (*i.e.* great  $T$ ) stochastic time evolution<sup>5</sup> (in the following, however, we will suppress any reference to the stochastic time  $t$ ). Also, one should keep in mind that the formula is to be intended as an *order by order* relation: in a sense, it is a shortening notation for a tower of relations, one for each perturbative order. Finally, it is worth pointing out that the  $p$  in  $M_{\alpha\eta}^{-1}(p, p)$  is now an index. The (diagonal) matrix elements of the inverse matrix are obtained by inverting the Dirac operator  $M$  on a  $\delta$ -like vector and then computing the scalar product with another  $\delta$ -like vector. More precisely, the vectors involved are what are usually termed *spin-color* vectors, with indexes referring to momentum, Dirac polarization and color. In order to keep the notation a bit lighter, we keep on omitting the color indexes. Within this (shortening) notation the relevant scalar product is

$$M_{\alpha\eta}^{-1}(p, p) = \sum_{\sigma\tau; q, t} \xi_{\sigma}^{(\alpha; p)}(q) M_{\sigma\tau}^{-1}(q, t) \xi_{\tau}^{(\eta; p)}(t) \quad \xi_{\delta}^{(\gamma; t)}(s) = \delta_{\gamma\delta} \delta_{ts} \quad (13)$$

Having performed the configuration average, we also average over all the components which are connected by hypercubic symmetry transformations. After that, we numerically invert the propagator to finally obtain the vertex function. It is worth stressing that also this inversion is a (matrix) order by order operation. We now have the self energy  $\Sigma(\hat{p}, \hat{m}_{cr}, \beta^{-1})$  at hand, from which we can extract the RC  $Z_q$  defined in Eq. (5) from the component  $\Sigma_V(\hat{p}, \hat{m}_{cr}, \beta^{-1})$ , which can in turn be extracted by taking traces.

Having to extract the RC  $Z_q$  in the continuum limit, this is the right time to restore physical dimensions, a process which enables us to single out irrelevant contributions. Consider

---

<sup>5</sup>To be even more precise, we should remark that our procedure also requires to compute time averages with different time discretization steps and then to extrapolate to the continuum-time limit.

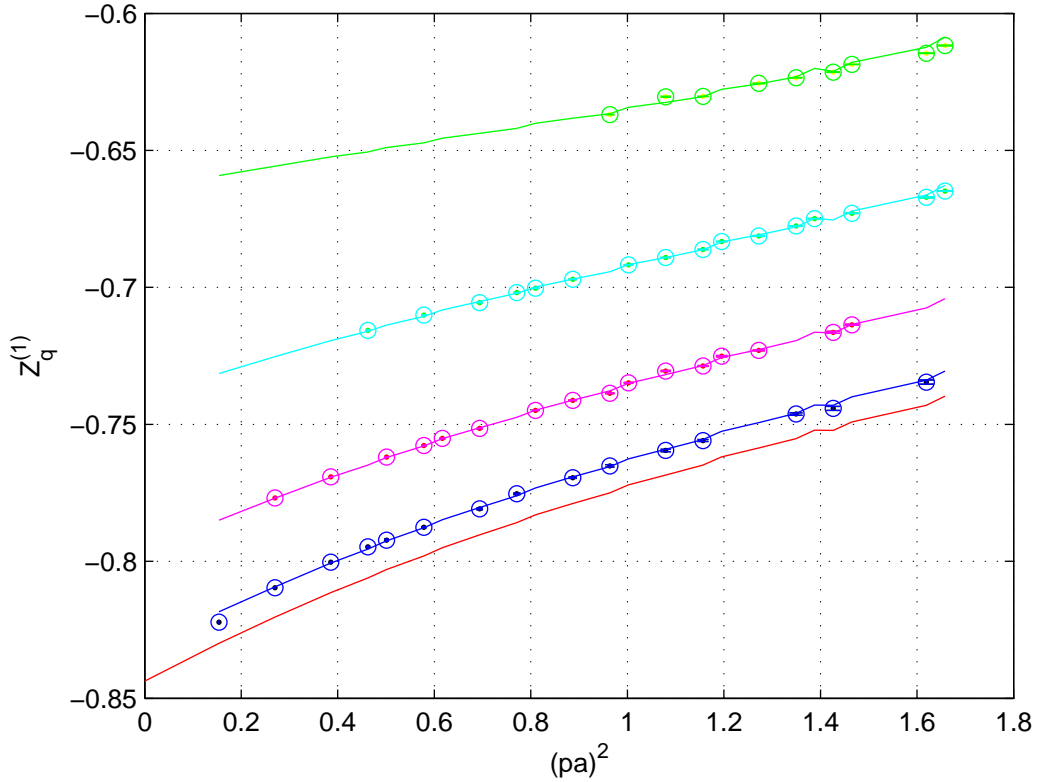


Figure 1: The continuum-limit extrapolation of  $Z_q^{(1)}$  (first loop of the quark field renormalization constant). The value one is interested in is the intercept at  $(pa)^2 = 0$ , reached on the lowest line, which is the contribution  $\Sigma_V^{(0)}(\hat{p}, \hat{m}_{cr}, \beta^{-1})$  in Eq. (14).

a *particular* direction  $\mu$  (*i.e.* in the following formula no summation over repeated indexes is assumed). The expected form of the self energy along  $\gamma_\mu$  is

$$i \gamma_\mu p_\mu \left( \Sigma_V^{(0)}(\hat{p}, \hat{m}_{cr}, \beta^{-1}) + \hat{p}_\mu^2 \Sigma_V^{(1)}(\hat{p}, \hat{m}_{cr}, \beta^{-1}) + \hat{p}_\mu^4 \Sigma_V^{(2)}(\hat{p}, \hat{m}_{cr}, \beta^{-1}) + \dots \right). \quad (14)$$

Having restored physical dimensions, for the first time the (physical) momentum  $p_\mu$  appears in front of the expression. The crucial observation is that  $\hat{p}_\mu$  is not the only vector at our disposal: having broken the symmetry to the hypercubic group, any  $\hat{p}_\mu^n$  can multiply  $\gamma_\mu$ . Invariance under reflections finally selects the relevant powers. Notice that restoring physical dimensions  $p_\mu$ , which is factored in front, is the only dimensionful momentum: other powers remain with a *hat* on top of them, *i.e.* they are *irrelevant* contributions vanishing in the continuum limit. To gain insight, the natural expression to look at is the tree-level quark propagator. Take the familiar expression  $2 \gamma_\mu \sin(\frac{\hat{p}_\mu}{2})$  and expand it: the only difference here is that the  $\Sigma_V^{(i)}(\hat{p}, \hat{m}_{cr}, \beta^{-1})$  are functions of  $\hat{p}$  themselves. More precisely, they are scalar functions. Performing a *hypercubic-invariant Taylor expansion* means writing them as polynomials in the invariants of the hypercubic group. This is a fitting procedure enabling us to reach the continuum limit, *i.e.* to single out the constant term in  $\Sigma_V^{(0)}(\hat{p}, \hat{m}_{cr}, \beta^{-1})$ . In Figure 1 one can inspect this process of taking the continuum limit (we plot what is embraced in parenthesis in Eq. (14)). Our final goal is given by the intercept of the lowest curve at

$\hat{p}^2 = 0$ : everything else does not survive the continuum limit. Notice that data arrange themselves in *families* of curves, depending on the different lengths of the component of  $p$  along  $\gamma_\mu$ . We choose to plot data versus  $\hat{p}^2$ , but one should keep in mind that this is not the only invariant the  $\Sigma_V^{(i)}(\hat{p}, \hat{m}_{cr}, \beta^{-1})$  can depend on. Our numerical result reproduces very well the analytical one.

## 5 Results

In the previous section we saw an example in which there was no anomalous dimension to deal with. This is of course also the case for finite RC ( $Z_V$  and  $Z_A$ ) or finite ratios ( $Z_P/Z_S$  and  $Z_V/Z_A$ ). In the following we present our results for these quantities. We computed at every order the relevant expectations values dictated by Eq. (1) and, having at hand the computation of the propagator, we followed the steps of amputation and projection on tree level structure. We could thus get the order-by-order expansions of the  $O_\Gamma(pa)$ 's in terms of which RC are defined. One-loop analytical results are well reproduced [14].

In the last subsection our results for the critical mass are presented.

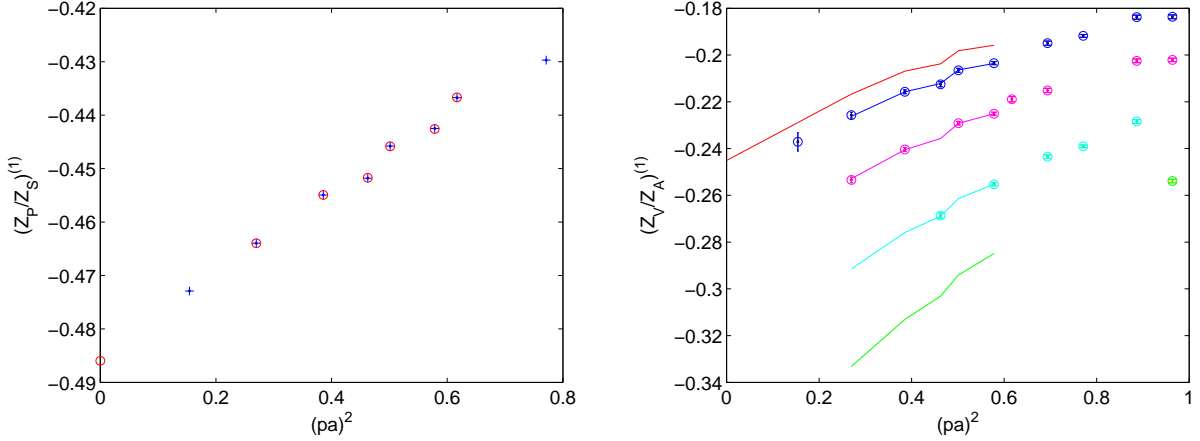


Figure 2: Computation to one loop of finite ratios of renormalization constants:  $Z_P/Z_S$  (left) and  $Z_V/Z_A$  (right). Data points taken into account in these particular fits are enclosed in circles (left) or joined by solid lines (right; see caption of Fig. 1).

### 5.1 The finite ratios $Z_P/Z_S$ and $Z_V/Z_A$

The ratios  $Z_P/Z_S$  and  $Z_V/Z_A$  are safely computable at every order. This simply means to take (again, order by order) ratios of  $O_\Gamma(pa)$  quantities. The quark field renormalization constant present in Eq. (4) drops out in the ratios, together with the divergence that affects  $Z_P$  and  $Z_S$  separately. In the end, one is left with the same situation we saw in the previous section: we simply have to perform at every order *hypercubic-invariant Taylor expansions* to

get the continuum-limit coefficients of the expansions. One-loop examples are presented in Fig. 2. Fitting a scalar quantity like  $Z_P/Z_S$  is actually easier (there is no direction singled out and consequently only one function, to be fitted as a polynomial in the hypercubic invariants).

We could perform many checks on our results. Finite-size effects are well under control, as checked by comparing results on  $16^4$  and  $32^4$  lattices in the quenched case. In the next section we will elaborate on computations for which this is not the case. We also stress that we can compute both  $Z_A/Z_V$  and  $Z_V/Z_A$ ; in the same way, we can compute both  $Z_P/Z_S$  and  $Z_S/Z_P$ . Due to the order-by-order nature of the computation, this is not a tautology: different ratios come from different (although correlated) combinations of data. We checked that to a very good precision the series obtained are inverse of each other.

Table 1 collects our results for different numbers of flavors. In the case  $n_f = 2$  four-loop results are available. As already pointed out, the fact that we were able to go one loop higher is due to our better knowledge of the three-loop critical mass in the  $n_f = 2$  case. Statistics in the cases  $n_f = 3, 4$  is actually poorer. The fact that we could anyway go to three loops is a numerical accident: the signals for these ratios are actually very clean.

$Z_P/Z_S$				
$n_f$	$O(\beta^{-1})$	$O(\beta^{-2})$	$O(\beta^{-3})$	$O(\beta^{-4})$
0	- 0.487(1)	- 1.50(1)	- 5.72(3)	n.a.
2	- 0.487(1)	- 1.46(1)	- 5.35(3)	- 21.6(3)
3	- 0.487(1)	- 1.43(1)	- 5.13(3)	n.a.
4	- 0.487(1)	- 1.40(1)	- 4.86(3)	n.a.
$Z_V/Z_A$				
$n_f$	$O(\beta^{-1})$	$O(\beta^{-2})$	$O(\beta^{-3})$	$O(\beta^{-4})$
0	- 0.244(1)	- 0.780(5)	- 3.02(2)	n.a.
2	- 0.244(1)	- 0.759(5)	- 2.83(2)	- 11.5(2)
3	- 0.244(1)	- 0.744(6)	- 2.72(2)	n.a.
4	- 0.244(1)	- 0.732(6)	- 2.57(2)	n.a.

Table 1: The ratios  $Z_P/Z_S$  and  $Z_V/Z_A$  for various number of flavor  $n_f$ . Four-loop results are only available for  $n_f = 2$ .

Having results for various numbers of flavors one can proceed to fit the  $n_f$ -dependence. Since the polynomial dependence on  $n_f$  of every order is fixed, this is another test for our results (see Fig. 3). We got

$$(Z_P/Z_S)^{(2)} = -1.50(1) + 0.0249(2) n_f \quad (Z_P/Z_S)^{(3)} = -5.72(3) + 0.151(5) n_f + 0.0159(5) n_f^2$$

$$(Z_V/Z_A)^{(2)} = -0.780(5) + 0.0121(1) n_f \quad (Z_V/Z_A)^{(3)} = -3.02(2) + 0.073(2) n_f + 0.098(3) n_f^2$$

Presented in this (more universal) way the precision of our results appears a bit poorer. As expected, results are strongly dominated by quenched contributions.

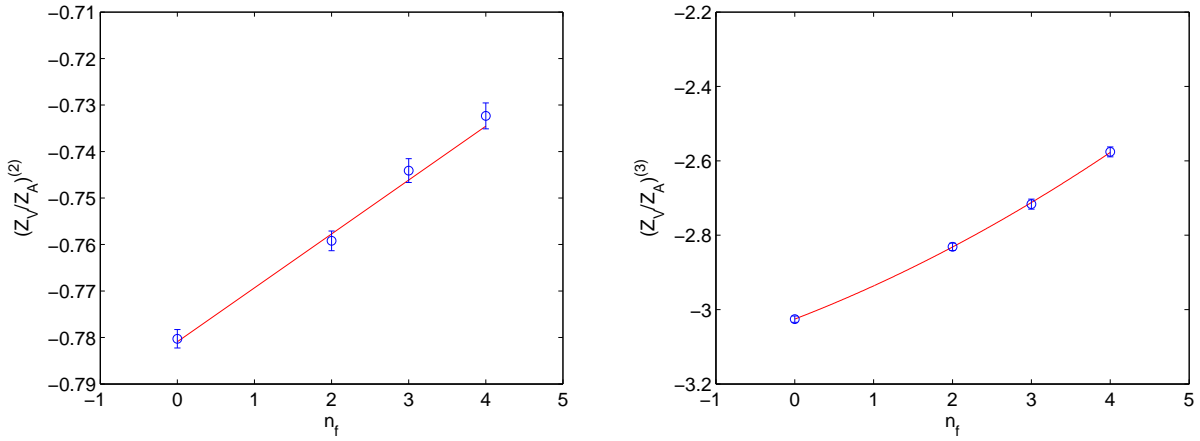


Figure 3: The  $n_f$  dependence of the ratio  $Z_V/Z_A$  at two (left, linear fit) and three (right, quadratic fit) loops.

## 5.2 $Z_V$ and $Z_A$

One loop examples of computations of  $Z_V$  and  $Z_A$  are plotted in Fig. 4.  $Z_V$  and  $Z_A$  are finite quantities by themselves. In our master formula Eq. (4) they are interlaced with log's coming from the quark field renormalization constant. The latter can be eliminated in two different ways. A first strategy is to cancel  $Z_q$  directly from the measurements of the propagator. Another possibility is to take ratios with the conserved vector current: this is just what we did in the case of  $Z_P/Z_S$  and  $Z_V/Z_A$ , this time having one of the  $Z$ 's equal to one. Both procedures return consistent results, which are summarized in Table 2, where we present results for  $n_f = 0, 2$  (also in this case, four-loop results are available for  $n_f = 2$ ).

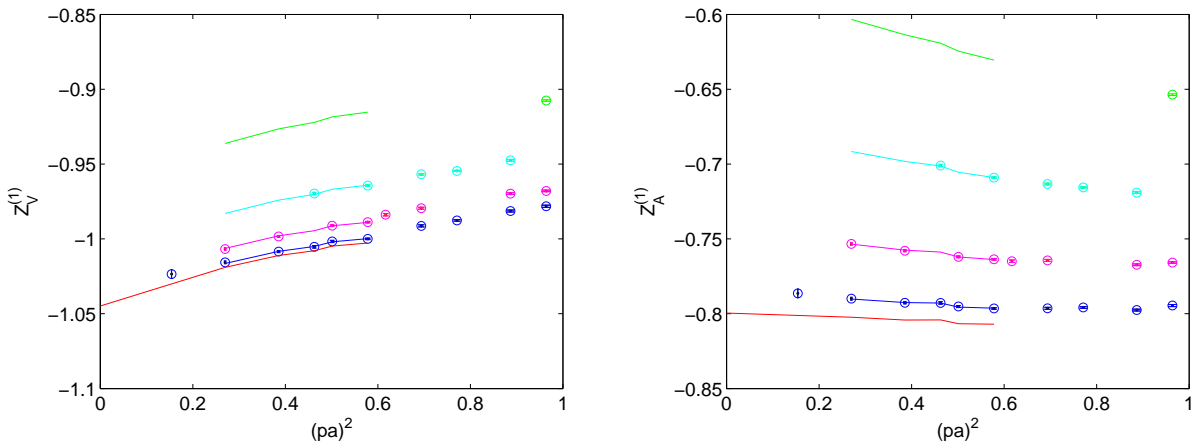


Figure 4: Computation to one loop of finite renormalization constants:  $Z_V$  (left) and  $Z_A$  (right). Same notations as in Fig. 2.

We have just discussed the two different approaches we used to compute  $Z_V$  and  $Z_A$ .

$Z_V$				
$n_f$	$O(\beta^{-1})$	$O(\beta^{-2})$	$O(\beta^{-3})$	$O(\beta^{-4})$
0	- 1.044(2)	- 1.98(3)	- 6.10(8)	n.a.
2	- 1.044(2)	- 1.88(3)	- 5.42(8)	- 17.0(9)
$Z_A$				
$n_f$	$O(\beta^{-1})$	$O(\beta^{-2})$	$O(\beta^{-3})$	$O(\beta^{-4})$
0	- 0.800(2)	- 1.39(3)	- 4.04(4)	n.a.
2	- 0.800(2)	- 1.31(3)	- 3.50(8)	- 9.8(6)

Table 2: The finite renormalization constants  $Z_V$  and  $Z_A$  for  $n_f = 0, 2$ .

In the previous subsection we presented results for the ratio  $Z_V/Z_A$ , which can of course as well be computed from the computation of  $Z_V$  and  $Z_A$ . One can verify that all these measurements are very well consistent. Still, they are controlled by different numerical noise, so that (for example) a direct computation of the ratio  $Z_V/Z_A$  is viable for all the  $n_f$  we took into account, while this is not the case for  $Z_V$  and  $Z_A$  separately (as already stated, statistics for  $n_f = 3, 4$  is poorer). In the end, all these procedures differ from each other for different ways of fitting irrelevant contributions. Getting rid of irrelevant contributions to single out continuum-limit results is a key issue in our approach, and so consistency between all these computations is a good test for reliability of our results.

### 5.3 A by-product: the critical mass

Analytical computations of the critical mass are available up to two loops [12]. A three-loop computation in the  $n_f = 2$  case was reported by our group in [6]. Here we present three-loops result for other  $n_f$  and add a four loop result for  $n_f = 2$ . Results are collected in Table 3. They were obtained from the defining formula of Eq. (12) by fitting irrelevant contributions to  $\Sigma_c(\hat{p}, \hat{m}_{cr}, \beta^{-1})$ . Also in this case there was no log coming from an anomalous dimension: in this case there is a power divergence, in force of which a perturbative result is not to be taken as an accurate one. It is nevertheless valuable indeed to maintain massless our fermions, *i.e.* as a counterterm.

$m_{cr}$	$n_f = 0$	$n_f = 2$	$n_f = 3$	$n_f = 4$
$O(\beta^{-3})$	- 13.11(6)	- 11.78(5)	- 11.02(9)	- 10.24(9).
$O(\beta^{-4})$	n.a.	- 39.6(4)	n.a.	n.a

Table 3: Three-loop critical mass for various  $n_f$ ; a four-loop result is available for  $n_f = 2$ .

Also in this case, one can fit a generic  $n_f$  result

$$m_{cr}^{(3)} = -13.11(6) + 0.62(5) n_f + 0.024(9) n_f^2.$$

## 6 Dealing with anomalous dimensions

We anticipated that dealing with anomalous dimensions requires some extra care. In order to get some insight, we discuss a first example in which an anomalous dimension comes into place, *i.e.* the one-loop computation of  $Z_S$ . By specifying our master formula Eq. (4) to this case we can write

$$\left(1 - \frac{z_q^{(1)}}{\beta} + \dots\right) \left(1 + \frac{z_s^{(1)} - \gamma_s^{(1)} \log(\hat{p}^2)}{\beta} + \dots\right) \left(1 + \frac{O_s^{(1)}(\hat{p}^2)}{\beta} + \dots\right) \Big|_{p^2=\mu^2} = 1$$

in which we explicitly wrote both the constant and the logarithmic contributions to renormalization constants (the only log comes in this case from  $Z_S$  since one-loop quark-field anomalous dimension is zero in Landau gauge).  $O_s^{(1)}(\hat{p}^2)$  is what is actually numerically measured. At one-loop order we can solve the previous relation to

$$z_q^{(1)} - z_s^{(1)} = O_s^{(1)}(\hat{p}^2) - \gamma_s^{(1)} \log(\hat{p}^2). \quad (15)$$

The message from Eq. (15) is simple: we will first subtract the logarithmic contribution and then proceed to our *hypocubic-invariant Taylor expansion*. This is plotted in Fig. 5: upper data points are  $O_s^{(1)}(\hat{p}^2)$ , lower data points are the subtracted ones. We can see on the left of Fig. 5 that by going through this procedure we miss the analytical result. Notice that it looks like we were *subtracting too much*. To be definite, the subtracted data points bend quite a lot in the IR region. In the end, this does not come as a surprise: *RI'-MOM* is an infinite-volume scheme, but we are (necessarily) computing on a finite volume. Problems are in a sense expected in the IR region, in the form of *pL* effects, as we can infer by dimensional analysis. Since for  $n_f = 0$  we have both  $32^4$  and  $16^4$  data, we are in a position to verify whether this is the real issue.

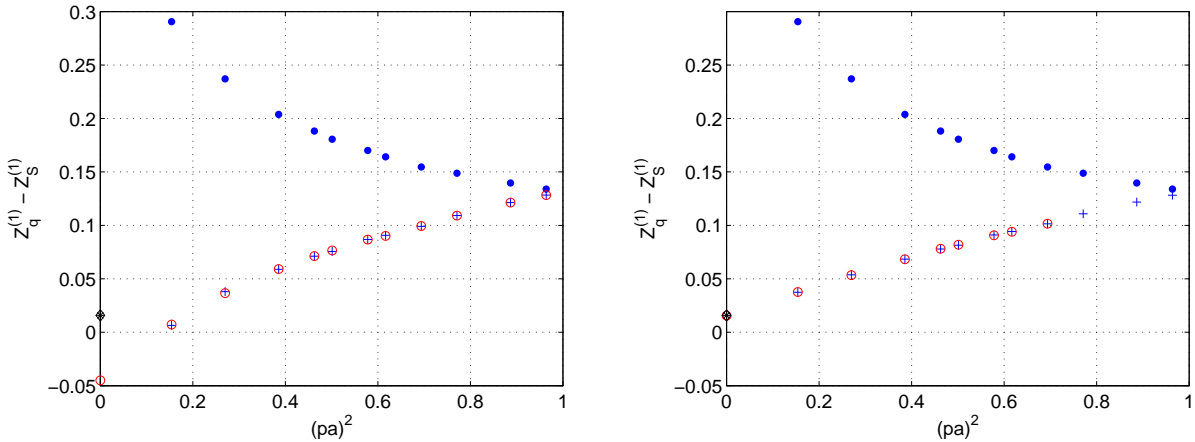


Figure 5: Computation of one loop renormalization constant for the scalar current. With respect to Eq. (15), upper points are the unsubtracted  $O_s^{(1)}(\hat{p}^2)$ , while lower (circled crosses) stand for the subtracted  $O_s^{(1)}(\hat{p}^2) - \gamma_s^{(1)} \log(\hat{p}^2)$ . Analytic result is marked with a darker symbol. On the left: no correction for finite volume. On the right: finite-volume *tamed-log* taken into account.

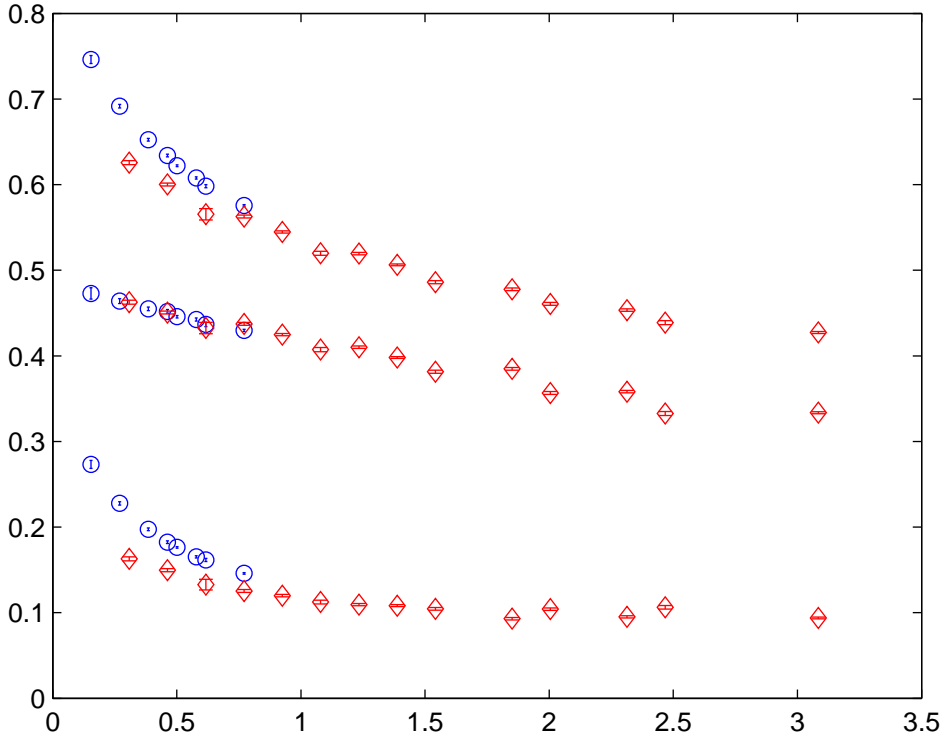


Figure 6: Computations of  $O_p^{(1)}(\hat{p}^2)$  (the equivalent of Eq. (15) for the pseudoscalar current) (top) and  $O_s^{(1)}(\hat{p}^2)$  (bottom) on  $32^4$  (circles) and  $16^4$  (diamonds). In the middle the ratio  $\frac{O_s^{(1)}(\hat{p}^2)}{O_p^{(1)}(\hat{p}^2)}$ , which appears safe with respect to finite-size effects.

Fig. 6 displays our results for  $O_p^{(1)}(\hat{p}^2)$  (the equivalent of Eq. (15) for the pseudoscalar current),  $O_s^{(1)}(\hat{p}^2)$  and of the ratio  $\frac{O_s^{(1)}(\hat{p}^2)}{O_p^{(1)}(\hat{p}^2)}$  on the two different volumes. While the ratio (in the middle of the figure) is safe (we have already made this point in the previous Section), quite remarkable finite-size effects are manifest for the  $O_i^{(1)}(\hat{p}^2)$ . It is obvious that by performing the subtraction of Eq. (15) on the  $16^4$  data points one misses the analytical result even more than in the left of Fig. 5. The picture stays much the same at higher loops.

Fig. 5 displays not only the problem (left), but also the way out (right). The correct result is reproduced if we subtract what we call a *tamed-log*, *i.e.* dressed with  $pL$  effects. The procedure we use to compute this function is inspired by the famous work of [15]. Suppose we want to compute a logarithmically divergent Feynman graph on a finite lattice. We can split it as in

$$I(p, a, L) = I(0, a, L) + (I(p, a, L) - I(0, a, L)) \equiv I(0, a, L) + J(p, a, L). \quad (16)$$

Being the divergence logarithmic and having subtracted  $I(0, a, L)$ ,  $J(p, a, L)$  is now UV finite, so that it can be computed in the continuum limit. In general, it will be now IR divergent, but this divergence (which in our case is regularized by finite volume) will be canceled by

contributions coming from  $I(0, a, L)$ , *i.e.*

$$\begin{aligned} I(0, a, L) &= c_1 + \gamma \log(a/L) + H(a/L) \\ J(p, a, L) &= c_2 + \gamma \log(pL) + F(pa, a/L) + G(pa, a/L, pL). \end{aligned} \quad (17)$$

We point out that  $I(0, a, L)$  can not contain  $pL$  effects: these should be looked for in  $J(p, a, L)$  and they will survive the process of taking the continuum limit ( $G(pa, a/L, pL) \rightarrow \tilde{G}(pL)$ ). In order to obtain the contribution which we called a *tamed-log* we just computed the relevant graph in the continuum limit on a finite volume. Notice that this function will approach a log for  $p \gg 1$ . As a matter of fact if one stays away from deep IR, the subtracted data points on the left and on the right of Fig. 5 are much the same. We stress that we are not saying that the finite size effects we have just elaborated on are the only ones. By inspection, they appear to be the relevant ones.

The situation is more complicate at higher loops and we will devote a separate paper to it [9].

## 7 Resumming the series

We now go back to the expansions of subsection 5.1 and 5.2 and try to resum them to obtain the finite RC's. Giving results and errors on top of them requires the estimation of truncation errors. We will in the following adopt the strategy of BPT. We stress from the very beginning that our real goal is the estimation of convergence properties of the series. It is only in force of the sufficiently high order of the expansions that one can hope to really gain insight. One should nevertheless be ready to accept that every statement on convergence will be decided on a strict case-by-case policy.

The different coupling constants we will use are all obtained in terms of the basic plaquette  $P$ . Let us define

$$x_0 = \beta^{-1} \quad x_1 \equiv \frac{\beta^{-1}}{\sqrt{P}} \quad x_2 \equiv -\frac{1}{2} \log(P) \quad x_3 \equiv \frac{\beta^{-1}}{P}. \quad (18)$$

$x_2$  and  $x_3$  are quite popular as boosted couplings. The reason why we also define  $x_1$  will be clear in a moment. Obtaining the expansions in  $x_i$  once the expansions in  $x_0$  are known is a textbook exercise, given the definitions in Eq. (18). One needs the expansion of the plaquette up to an order for which analytical results [16] are known. Only for  $n_f = 2$  one also needs the fourth order, which reads  $P = 1 + \dots + \beta^{-4} + \dots$

We resum the series at  $\beta = 5.8, n_f = 2$ . This makes possible a comparison with the non-perturbative results of [8].

Fig. 7 displays the resummation of  $Z_P/Z_S$  and  $Z_S/Z_P$  in the four different couplings. One can inspect from the very beginning the impact of a basic property of BPT which is often underestimated: all the couplings are equal at tree level, which means that all the expansion are equal at leading order. One loop BPT amounts to sitting on a straight line, whose slope is dictated by the one-loop coefficient. Only at higher loops we can gain some insight on

convergence properties. There is actually a variety of convergence patterns (taking also  $x_1$  into account is helpful with this respect).

In particular, one can check the following:

- Within a fixed definition of the coupling, convergence is of course better and better as the order increases. As common wisdom suggests, convergence in the bare coupling is not so brilliant and in general quite different convergence patterns are manifest; they appear quite satisfactory for  $x_2$  and  $x_3$ . In particular, for the case of  $x_2$  expansion we plot in Fig. 8 the deviations  $\Delta^{(N)}$ , defined as the differences between resummation at order  $N$  and resummation at order  $N - 1$ . The good scaling should not be taken too seriously (this is largely a numerical accident). Still, this is signaling a reasonable convergence pattern.
- As the order increases, expansions in different couplings get closer to each other, as expected; in particular expansions in  $x_2$  and  $x_3$  are quite close to each other.
- The resummed results for  $Z_P/Z_S$  and  $Z_S/Z_P$  in the  $x_2$  and  $x_3$  couplings are the inverse of each other to a reasonable accuracy. This is also a good indication.

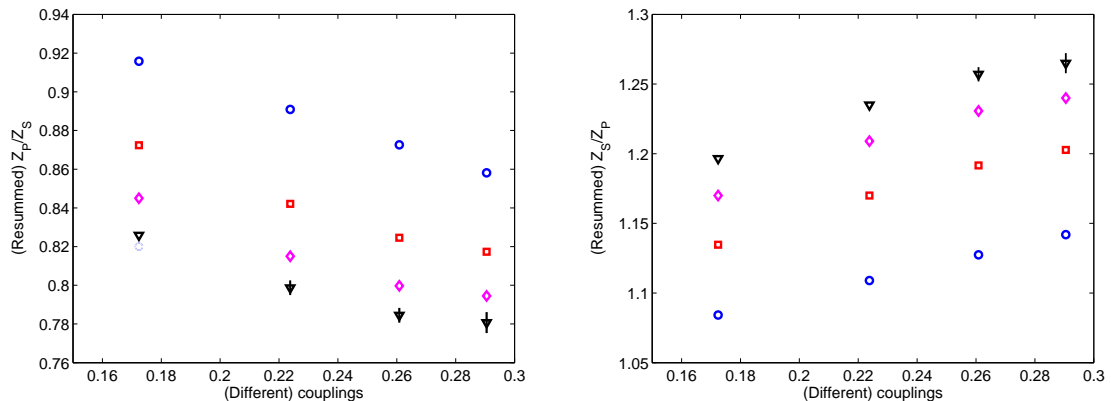


Figure 7: Resummations of  $Z_P/Z_S$  (left) and  $Z_S/Z_P$  (right) for  $n_f = 2$  at  $\beta = 5.8$  to one (circles), two (squares), three (diamonds) and four (triangles) loops (the last is the only one which has a sizeable error). We show resummations for different couplings: on the x-axis, the (different) values of the different couplings. From the left:  $x_0, x_1, x_2, x_3$  ( $x_0$  is  $\beta^{-1}$ , see text for the definitions of the other couplings).

Convergence properties of the expansions in the  $x_2$  and  $x_3$  couplings are good enough to extract a result. We notice that if one adds to the result at a given order the deviation from the immediately lower order, one always ends up at the same result (as a matter of fact a popular way to pin down a truncation error is just taken from deviations which we previously called  $\Delta_n$ ). We thus quote  $Z_P/Z_S = 0.77(1)$ .

We have already made the point that to assess convergence properties one should adopt a case by case strategy. This can be clearly seen when we proceed to resum  $Z_A$  and  $Z_V$ .

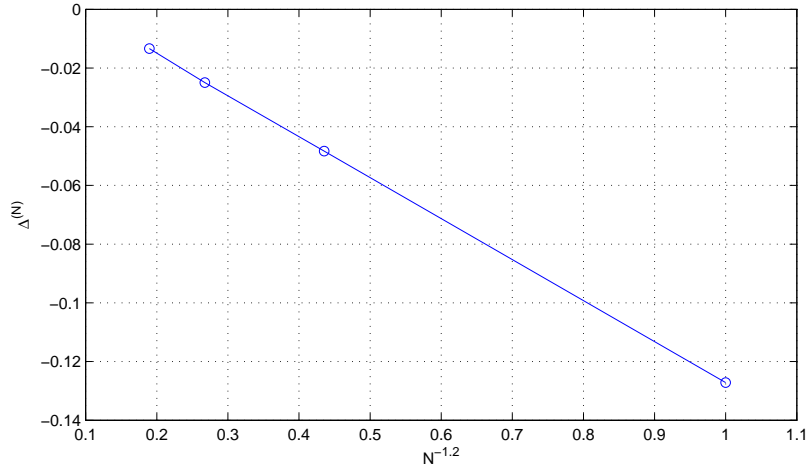


Figure 8: The scaling of deviations of different order truncations for the quantity  $Z_P/Z_S$  for the  $x_2$  coupling.

Before doing that, we give a trivial example of what a blind application of the idea of BPT can result in. In Fig. 9 we *exaggerate* the boosting of the coupling, by taking into account other coupling  $x_\alpha \equiv \frac{\beta^{-1}}{P^\alpha}$  ( $\alpha > 1$ ). As one can see, convergence properties are completely jeopardized.

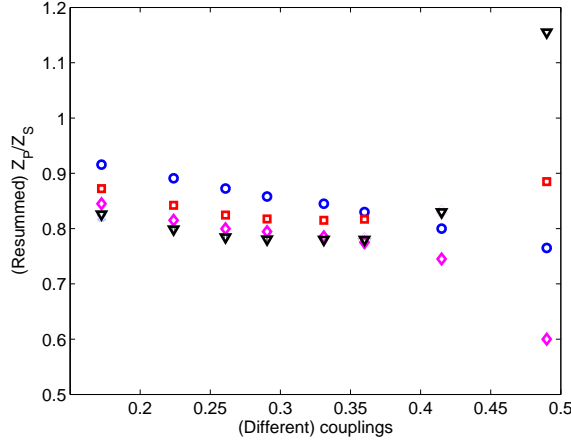


Figure 9: Resummations of  $Z_P/Z_S$  (left) for  $n_f = 2$  at  $\beta = 5.8$ . The same as in Fig. 7, but this time exaggerating the boosting of the couplings.

In Fig. 10 we plot the resummation of  $Z_V$  and  $Z_A$  (again, at  $\beta = 5.8, n_f = 2$ ). As one can see, this time convergence properties of the expansion in the bare coupling are not so bad. Consequently, one is already at risk of overshooting at one loop BPT and the expansions in  $x_2$  and  $x_3$  oscillate. Our final estimates are  $Z_A = 0.79(1)$  and  $Z_V = 0.70(1)$ .

Our resummed results are quite consistent with [8]. A bigger deviation is seen on the

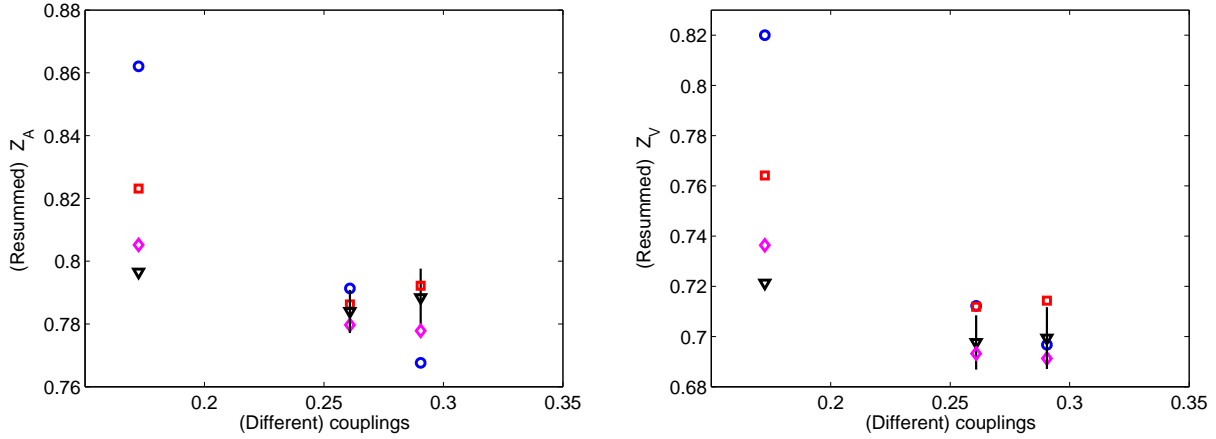


Figure 10: Resummations of  $Z_A$  (left) and  $Z_V$  (right) for  $n_f = 2$  at  $\beta = 5.8$  to one (circles), two (squares), three (diamonds) and four (triangles) loops (the last is the only one which has a sizeable error). We show resummations for different couplings: on the  $x$ -axis, the (different) values of the different couplings. From the left:  $x_0$ ,  $x_2$ ,  $x_3$  (see text for the definitions of the couplings).

values of  $Z_A$  and  $Z_V$ . To our understanding this could be mainly inputed to indeterminations coming from the chiral extrapolation.

## 8 Conclusions

We presented high-order computation of renormalization constants for Lattice QCD. Finite-size effects are well under control for the quantities we considered. There is no extrapolation involved in staying at the chiral limit in which renormalization conditions are imposed. The continuum limit extraction is achieved in a clean way. Truncation errors can be well assessed by a judicious use of BPT. Thus, the main message of this paper is that high precision perturbative computations of lattice QCD renormalization constants are feasible and should not be regarded necessarily as a second choice.

Further work will follow, both to complete the job for logarithmically divergent quantities and to take into account different actions (in particular different fermionic regularizations). This is not expected to imply any change in strategy and the implementation is mainly a matter of programming. In particular, work has already started to extend results to Clover fermions and to other gauge actions.

## Acknowledgments

We warmly thank Andrea Mantovi for having collaborated with us at an early stage of this project. We are very grateful to V. Lubicz and C. Tarantino for many stimulating discussions and for sharing with us their data. We also acknowledge interesting discussions with S. Capitani. F.D.R., V.M. and C.T. acknowledge support from both Italian MURST under contract 2001021158 and from I.N.F.N. under i.s. MI11. L.S. has been partially supported by DFG through the Sonderforschungsbereich 'Computational Particle Physics' (SFB/TR 9).

## References

- [1] For a beautiful review on LPT see S. Capitani, *Lattice Perturbation Theory*, Phys. Rep. 382 (2003) 113 [hep-lat/0211036].
- [2] G.P. Lepage and P.B. Mackenzie, *On the viability of Lattice Perturbation Theory*, Phys. Rev. D 48 (1993) 2250 [hep-lat/9209022].
- [3] M. Constantinou, H. Panagopoulos and A. Skouroupathis, Phys. Rev. D **74** (2006) 074503 [arXiv:hep-lat/0606001].
- [4] G. Martinelli, C. Pittori, C.T. Sachrajda, M. Testa and A. Vladikas, *A general method for non perturbative renormalization of lattice operators*, Nucl. Phys. B 445 (1995) 81 [hep-lat/9411010].
- [5] M. Luescher, R. Narayanan, P. Weisz and U. Wolff, *The Schroedinger functional: a renormalizable probe for non abelian gauge theories*, Nucl. Phys. B 384 (1992) 168 [hep-lat/9207009].
- [6] F. Di Renzo and L. Scorzato, *Numerical Stochastic Perturbation Theory for full QCD*, JHEP 04 (2004) 073 [hep-lat/0410010].
- [7] G. Parisi and Wu, *Perturbation Theory without Gauge Fixing*, Sci. Sin. 24 (1981) 35.
- [8] D. Becirevic, B. Blossier, Ph. Boucaud, V. Gimenez, V. Lubicz, F. Mescia, S. Simula and C. Tarantino, *Non perturbatively renormalized light quark masses with two dynamical fermions*, PoS(Lat2005)079 [hep-lat/0509091].
- [9] F. Di Renzo, V. Miccio and C. Torrero, *High-loop perturbative renormalization constants for Lattice QCD (II): logarithmically-divergent constants for Wilson quark currents*, in preparation.
- [10] W. Celmaster and R. J. Gonsalves, *The renormalization prescription dependence of the QCD coupling constant*, Phys. Rev. D 20 (1979) 1420.
- [11] J.A. Gracey, *Three loop anomalous dimension of non-singlet quark currents in the RI' scheme*, Nucl. Phys. B 662 (2003) 247 [hep-ph/0304113].

- [12] E. Follana and H. Panagopoulos, *The critical mass of Wilson fermions: a comparison of perturbative and Monte Carlo results*, Phys. Rev. D 63 (2001) 017501 [hep-lat/0006001];  
 S. Caracciolo, A. Pelissetto and A. Rago, *Two-loop critical mass for Wilson fermions*, Phys. Rev. D 64 (2001) 094506 [hep-lat/0106013].
- [13] F. Di Renzo, M. Laine, V. Miccio, Y. Schroder and C. Torrero, *The leading non-perturbative coefficient in the weak-coupling expansion of hot QCD pressure*, JHEP **0607** (2006) 026 [arXiv:hep-ph/0605042].
- [14] G. Martinelli and Yi-Cheng Zhang, *The connection between local operators on the lattice and in the continuum and its relation to meson decay constants*, Phys. Lett. B 123 (1983) 433.
- [15] H. Kawai, R. Nakayama and K. Seo, *Comparison Of The Lattice Lambda Parameter With The Continuum Lambda Parameter In Massless QCD*, Nucl. Phys. B **189**, 40 (1981).
- [16] B. Alles, A. Feo and H. Panagopoulos, *Asymptotic scaling corrections in QCD with Wilson fermions from the 3-loop average plaquette*, Phys. Lett. B **426** (1998) 361 [Erratum-ibid. B **553** (2003) 337] [arXiv:hep-lat/9801003].